Proceedings of the 28th International Conference on Offshore Mechanics and Arctic Engineering
OMAE2009
May 31-June 5, 2009, Honolulu, Hawaii

OMAE2009-80222

FATIGUE YIELD OF SHIP STRUCTURES

Kalman Žiha
Department of Naval Architecture and Ocean Engineering
Faculty of Mechanical Engineering and Naval Architecture
University of Zagreb, Zagreb, Croatia

Branko Blagojević
Department of Naval Architecture
Faculty of Electrical and Mechanical Engineering and Naval Architecture
University of Split, Split, Croatia

ABSTRACT

The paper on the first place summarizes the fatigue yield approach as a cause-effect interaction between fatigue damage progression and fatigue endurance. Secondly it investigates the fatigue strength worsening on experimental S-N data and the load variability effects in shipbuilding. Next it applies the Classification Society's rule-based procedure for fatigue analysis of ship's structure that uses a simplified fatigue strength assessment method. The example elaborates fatigue yield effect on the seagoing operation of a double hull 47400 tdw tanker. At the end the paper recommends the procedure for assessment of ship lifetime shortening due to the fatigue yielding under constant and variable amplitude block loadings.

INTRODUCTION

The damage progression theories have been leading fatigue research in engineering since the linear damage rule (LDR) has come into wide application, e.g. review by Fatemi and Yang [1]. Therefore, the non-linear fatigue yield approach adapts to the practical engineering methods in fatigue analysis such as the basic linear damage rule by Palmgren [2] and Miner [3] and to the non-linear Marco-Starkey model [4].

The fatigue yield is regarded in the study as a damage-endurance interaction and fatigue strength worsening that causes fatigue life shortening under intermittent block loadings with respect to the LDR. Thus the Fatigue Yield Rule (FYR) [5] basically takes up the results of LDR and then modifies the primary linear damage accumulation results for the yielding effect using the same set of experimental data.

The FYR indicates in the paper how the fatigue life shortens due to the yield of critical details [6, 7, 8] with respect to the LDR. The example applies Classification rules [9, 10] based on LDR and uses FYR to assess the fatigue life of a tanker [11] also accounting for the load variability effects.

DAMAGE PROGRESSION

The Palmgren-Miner [2, 3] linear rule estimates the cumulative fatigue damage $D(k)$ up to k block loadings by summing up all contributing damage fractions. Damage fractions $D_{j/i}$ are taken as the cyclic ratio $r_{j/i}=n_j/N_i$ under j^{th} loading block of n_j loading cycles for i^{th} constant amplitude stress $\Delta\sigma_i$ also relating to the appropriate fatigue lifetime N_i. The LDR defines the cumulative fatigue damage as follows:

$$D(k) = \sum_{j=1}^{k} r_{j/i} \tag{1}$$

The Marco-Starkey model [4] introduces the exponential relation on accumulating damage fractions into (1) as shown:

$$D(k) = \sum_{j=1}^{k} r_{j/i}^{\alpha} \tag{2}$$

The fatigue yield rate also apt as a yield factor y_i relates the general fatigue damage progression rate (DPR) in the form $dD_{j/i}/dn_j$ [12] to the linear damage progression rate (LDPR) defined as $1/N_i$ [3] that is taken as granted in LDR for each i^{th} load in the following general form:

$$\frac{dY_{j/i}}{dD_j} = y_i = \left(\frac{dD_{j/i}}{dn_j}\right) \Big/ \left(\frac{1}{N_i}\right) \tag{3}$$

The yield factor y_i in (3) corrects the LDR (1) for the effect of yielding under stress amplitude $\Delta\sigma_i$ as shown:

$$D'(k) = \sum_{j=1}^{k} y_i \cdot r_{j/i} \tag{4}$$

An overall correction factor Y can substitute yield factor y_i to approximate (4) in exponential or in linear form as follows:

$$D'(k) = \left[Y \cdot D(k)\right]^{\alpha} \approx Y \cdot D(k) \tag{5}$$

FATIGUE YIELD

The theoretical fatigue yield model [5] takes the formerly accumulated successive fatigue damage fractions $D_{j/i}$ for all i stress amplitude $\Delta\sigma_i$ up to the $(j-1)^{th}$ loading block, Fig. 1, as the measure of fatigue strength worsening:

$$W_j = \sum_{i=1}^{j-1} D_{j/i} = D_i(j-1) \tag{6}$$

The damage progression affects the endurance reduction, Fig. 1, as it is presented next:

$$E_j = 1 - D_i(j-1) \tag{7}$$

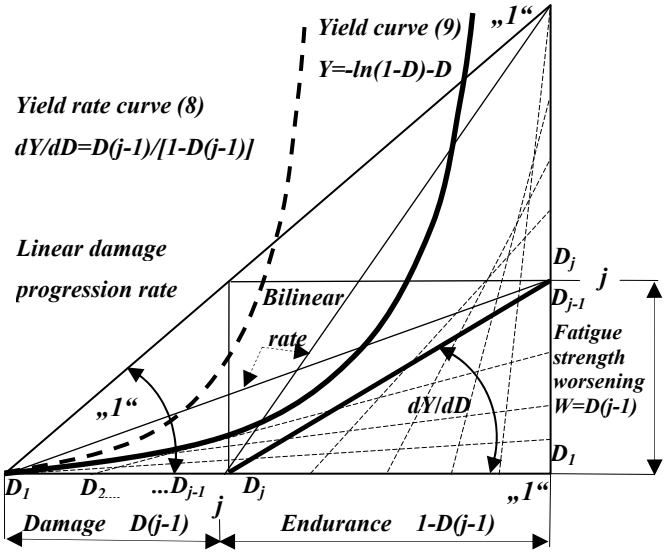

Figure 1. Damage progression and fatigue yield model [5]

Consequently the fatigue yield rate relates recursively the accumulated strength worsening W_j (6) to the endurance reduction E_j (7) in a generalized form as follows:

$$\frac{dY_j}{dD_i} = \frac{W_j}{E_j} = y_j = \frac{(\varphi+\delta) - \delta \cdot D_i(j-1)}{1 - D_i(j-1)} \tag{8}$$

Thus the integral of (8) indicates the logarithmic and the linear components of the fatigue yield $Y(D)$, Fig. 1, as follows:

$$Y(D) = \sum_{j=1}^{k} y_j \cdot D_{j/i} = \int_0^D \frac{dY}{dD} dD = -\varphi \cdot \ln(1-D) + \delta \cdot D \tag{9}$$

The fatigue yield intensity factor δ in (8, 9) influences the linear part of (9) and the factor φ expresses the initial propensity to fatigue yield [5] that affects the nonlinear part of (9), Fig. 2.

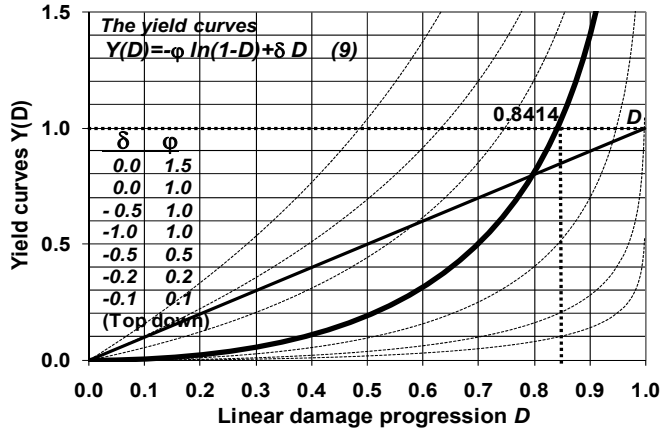

Figure 2. Yield curves for different parameters δ and φ

LOAD AMPLITUDE VARIABILITY FACTOR

Socha [12] used the method based on the observations of the inelastic strains during the fatigue test on steel specimens under fully reversible load to assess the general damage progression rate DPR $dD_{j/i}/dn_j$. According to Johannesson and Svensson [13] variable amplitude load fatigue tests methodologies are available but data are rare and involve additional uncertainties.

The relation (3) of the DPR of variable stress amplitude data to the linear damage progression rate LDPR of constant stress amplitude data expresses a load amplitude variability factor for stress amplitude $\Delta\sigma_i$ denoted herein as v_i. For steels A336GR5 and A387GR22 Socha [12] v_i are given on Fig. 3.

The load variability factor allows the assessment of the fatigue damage fraction under j^{th} variable loading block for i^{th} stress amplitude $\Delta\sigma_i$ with respect to constant loads appropriate to LDR for belonging fatigue lifetime N_i, Fig. 3, as shown:

$$D'_{j/i} = v_i \cdot D_{j/i} \tag{10}$$

The cumulative damage up to k^{th} block of each variable stress amplitude load $\Delta\sigma_i$ for all i is then:

$$D'(k) = \sum_{j=1}^{k} v_i \cdot D_{j/i} \tag{11}$$

The reported results of laboratory fatigue experiments on steel under variable amplitude loads by Socha [12] indicate that the load variability factors for two types of steels depends on the applied load amplitudes, Fig. 3. The approximation as in (5) can benefit from piece-wise linearization of load variability factors for the expected range of stress amplitudes (shaded stripes on Fig. 3, as shown:

$$D'(k) \approx V \cdot D(k) \tag{12}$$

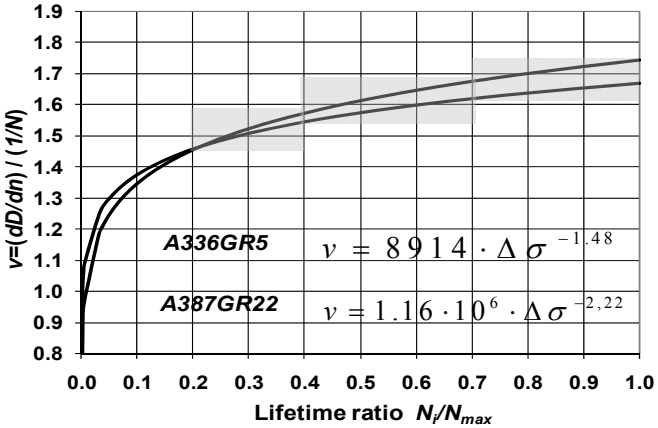

Figure 3. Load amplitude variability factor v [5,12]

FATIGUE YIELD OF WELDED JOINTS

For practical purposes the S-N fatigue test data for welded joints in shipbuilding [9, 10], Fig. 4, supported by the IIW [6], also by (ECCS) Fatigue Recommendations [7] and Eurocode 3 [8] are given by the fatigue strength and life relation as shown:

$$\frac{\Delta\sigma_i}{\Delta\sigma_R} = \left(\frac{N_i}{N_R}\right)^{-1/m} \tag{13}$$

The paper applies the fatigue yield approach (8, 9) on fatigue strength worsening analysis of families of IIW [6, 9] S-N fatigue strength reference values (13), Fig. 4, used in shipbuilding (detail categories - having the same fatigue resistance) for different welded specimens.

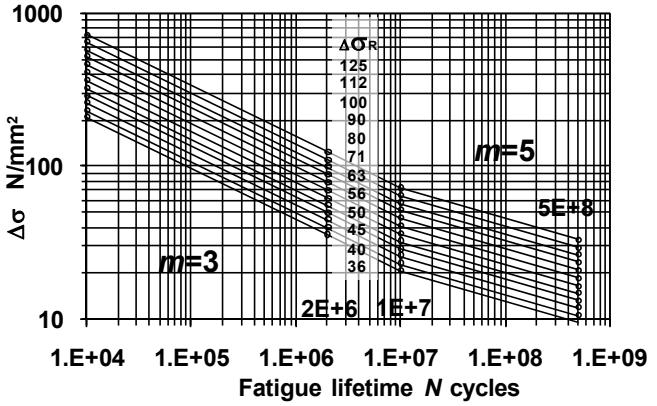

Figure 4. IIW S-N curves [6, 9] for detail categories 36-125

Each of the R^{th} detail categories $\Delta\sigma_R$ of 36, 40, 45, 50, 56, 63, 71, 80, 90, 100, 112, 125 and so on, in MPa, correspond to the fatigue reference life at $N_R=2\cdot10^6$ cycles. The fatigue life under variable stress amplitude according to Rule recommendation [9] for m=3 ranges up to $N_{max}=1\cdot10^7$, Fig. 4.

The fatigue yield approach applied to S-N data considers that the strength worsening $\boldsymbol{W=\Delta\sigma_i\ (1\text{-}D)^{-1/m}}$ reduces the lifetime N_i in proportion to the damage progression $\boldsymbol{D_{j/i}=n_j/N_i}$. Thus the fatigue yield rate is $\boldsymbol{dD'/dD=W/d\sigma=(1\text{-}D)^{-1/m}}$.

Fatigue yielding based on S-N data represents the fatigue strength worsening due to earlier accumulated damages with respect to an intact specimen as used by LDR [5], Fig. 5, as:

$$D'(D)=\int_0^D \frac{dD'}{dD}dD=\alpha\cdot\frac{m}{m-1}\cdot\left[1-(1-\alpha\cdot D_{j/i})^{\frac{m-1}{m}}\right] \qquad (14)$$

Parameter α in (14) represents the fatigue yield intensity [5]. Particularly the fatigue yield for all IIW detail categories with inverse slope of m=3 [6] using (9 and 14), Fig. 5, is as shown:

$$D'(D)=\frac{3}{2}\cdot\left[1-(1-D)^{\frac{2}{3}}\right]\approx 1.24\cdot D \qquad (15a)$$

The theoretical fatigue yield (9) can also fit the strength worsening (15a) as follows:

$$Y(D)=-0.15\cdot\ln(1-D)+0.91\cdot D \qquad (15b)$$

Thus, welded joints for m=3 under block loads yield (15) about 24% faster of the linear damage progression. Consequently the fatigue life shortens due to worsening at 80.75% with respect to the linear damage progression, Fig. 5.

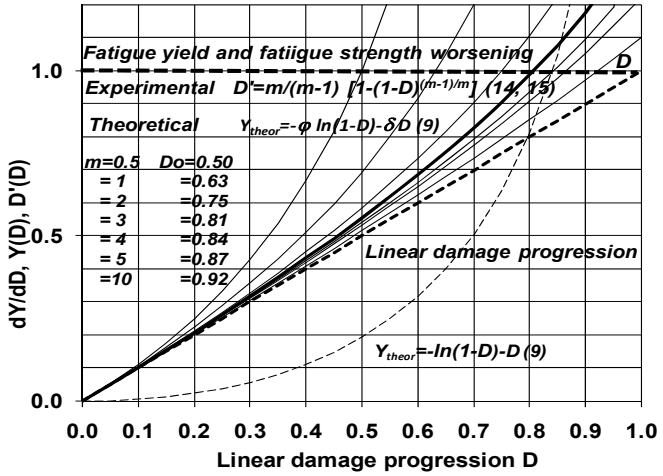

Figure 5. Fatigue strength worsening for IIW S-N curves

EXAMPLE

The illustrative example employs the Classification Society's-rule-based procedure [9] using a simplified fatigue strength assessment also described in [10] on a double hull tanker [11] built in Croatia with following particulars:

Chemical tanker	47400 tdw
Length overall	L_{oa} = 182.5 m
Length between perpendiculars	L_{pp} = 174.8 m
Rule (construction) length	L = 173.1 m
Breadth molded	B = 32.2 m
Depth molded	D = 17.5 m
Draught design	T = 11.0 m
Ballast draught	d_2 = 7.2 m
Maximum draught (full load)	d_1 = 12.2 m
Web frame spacing	S = 3.4 m
Block coefficient	C_b = 0.82
Maximum service speed	v = 15 kn,
Max. S.W.B.M., sagging (load manual)	296250 kNm
Section modulus at deck	W_D = 16.14 m^3
Section modulus at bottom	W_B = 21.25 m^3
Height of NL above base line	Z_{NL} = 7.55 m

According to Hansen and Winterstein [14] and ISSC Committee *Fatigue and Fracture* [15] about 40% of fatigue damages are located at connections of longitudinals to the transverse web frames. Most of the fatigue cracks were found at ship's sides close to the full and ballast draughts, Fig. 6.

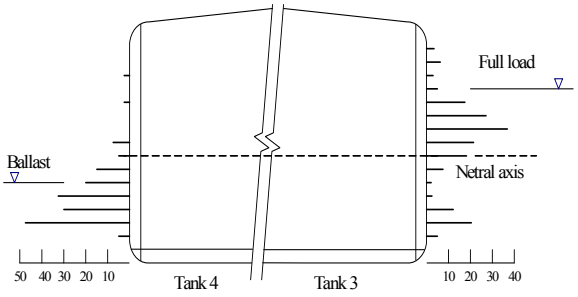

Figure 6. Number of cracks in tanker longitudinals [14,15]

Therefore, the next example investigates the fatigue yield of side transverse web stiffener end weldment at intersection of hull outer side longitudinal under lateral and in plane loads, Fig. 7. The selected detail 2 under consideration is located at midship section immediately below the ballast draught, Fig. 8.

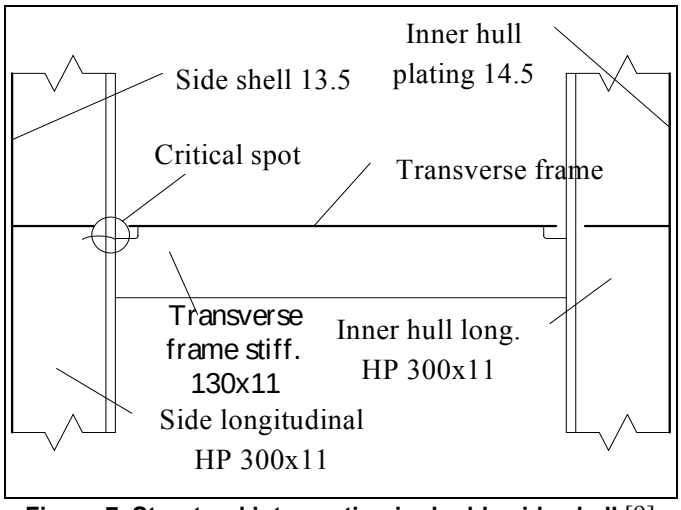

Figure 7. Structural intersection in double side shell [9]

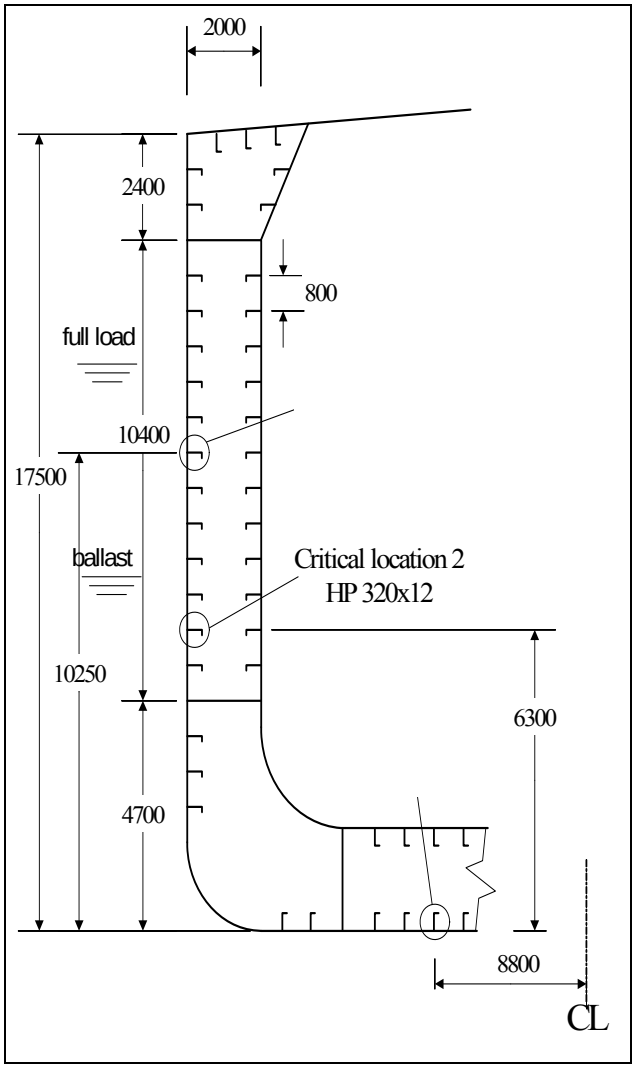

Figure 8. Location 2 of the structural detail

Rule based fatigue analysis by linear damage rule

The fatigue assessment rule based procedure [10] uses a nominal stress approach to beam theory under assumptions:

(a) a linear cumulative damage model has been used in connection with the S-N data.
(b) for stiffener end connections, nominal stresses are derived by empirical rule based loads.
(c) the long term stress ranges can be characterized by a modified Weibull probability distribution.
(d) the detail idealization and classification is based on joint geometry under simple loadings.
(e) the cumulative fatigue damage ratio, D, is to be less than 1 for the design life of the ship.
(f) the design life is not to be less than 25 years.

Table 1. Web stiffener end connection to side longitudinal

With heel stiffener [9]	HP longitudinal	$\Delta\sigma_R$
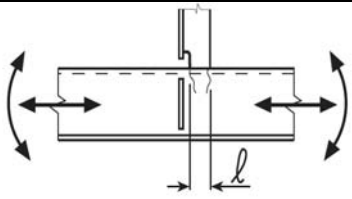	Direct connection	
	$\ell \le 150$:	56
	$\ell > 150$:	50

ASSESSMENT OF THE FATIGUE STRENGTH

The fatigue strength assessment implies three phases.

The calculation of stresses according to empirical formulae and Rule based loads

The rule based nominal seaway-induced stresses are calculated earlier [11]. The maxima of local stress ranges are assessed in full and ballast conditions for rule based number of cycles $N_R = 10^4$ for representative probability of $1/N_R = 10^{-4}$ as:

$\Delta\sigma_{Full}$=142N/mm^2 and $\Delta\sigma_{Ball}$=60N/mm^2.

The peak stress ranges for full and ballast loads define the A-type line spectrum for seagoing conditions, Fig. 9.

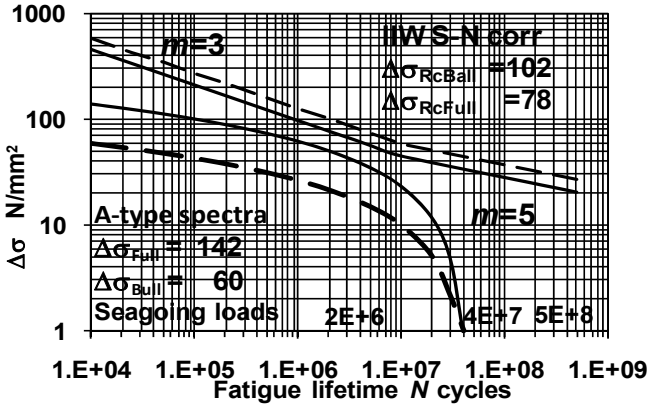

Figure 9. Seagoing-induced stresses-line spectrum type A

Selection of the design S-N curve

The example investigates the intersection of the transverse frame stiffener end and the side shell longitudinal, Fig. 7. The detail is on location 2 in the double hull outer side bellow the ballast draught, Fig. 8. The detail category $\Delta\sigma_R$ =56 N/mm^2, Fig. 4, is recommended for $\ell \le 150$ and for asymmetric HP section of longitudinal, Fig. 7, also Table 1 and Fig. 10 [9].

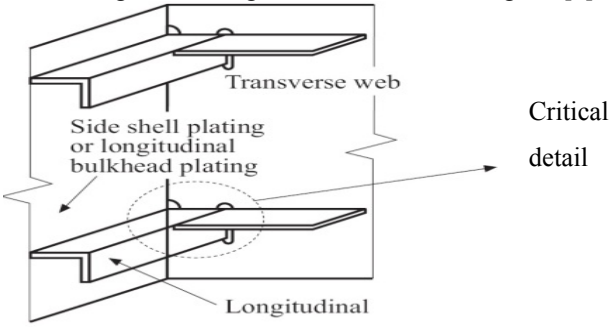

Figure 10. Mode of cracking at intersection

Since is the $\Delta\sigma_{Full}$>2.5$\Delta\sigma_R$=140N/mm^2 the fatigue strength analysis is required for welded structures of detail category below 80. The corrections of the primary strength reference values (or the detail category) are required by the rules [9] to account for other influences on the fatigue strength for full and ballast conditions, respectively, Fig. 9, as

$$\Delta\sigma_{Rc\,Full} = f_m \cdot f_R \cdot f_w \cdot f_i \cdot \Delta\sigma_R = 1 \cdot 1 \cdot 1.4 \cdot 1 \cdot 56 = 78\ N/mm^2$$

$$\Delta\sigma_{Rc\,Ball} = f_m \cdot f_R \cdot f_w \cdot f_i \cdot \Delta\sigma_R = 1 \cdot 1.3 \cdot 1.4 \cdot 1 \cdot 56 = 102\ N/mm^2$$

According the rules f_m counts for material effect, f_R for mean stress, f_w for weld shape (endings of stiffeners) and f_i for the importance of the weldment under consideration. Note that the critical detail is below the hull section neutral axes and therefore it is considered that it is under tension when fully loaded and under compression in ballast condition.

Calculation of the cumulative damage

The rule based procedures [9, 10] assume the long term distribution of stress ranges as a two-parameter Weibull distribution and use the closed-solution for Palmgren-Miner cumulative fatigue damage D_i for each i^{th} loading condition as:

$$D_i = \frac{n_s}{C}\frac{(\Delta\sigma_i)^m}{(\ln N_R)^{m/k}}\mu_i\Gamma(1+m/k) \qquad (16)$$

In (16) $n_s = f_0\ U/4logL = 0.75\text{x}10^8$ is the number of cycles for the expected design life. The value is generally between $0.6\text{x}10^8$ and $0.8\text{x}10^8$ cycles for a design life of 25years (supposedly in example are 2x15 alternating full/ballast voyages of 12 days per year) using f_0 =0.85 factor of non-sailing time and $U=0.7884\text{x}10^9$ design life in seconds/25years. $C_{full}=9.64\text{x}10^{11}$ and $C_{ball}=2.12\text{x}10^{12}$ – are calculated constants depending on corrected category for full and ballast conditions $\Delta\sigma_{RcFull}=78\ N/mm^2$ and $\Delta\sigma_{RcBall}=102\ N/mm^2$.

m=3 and 5 are the inverse slopes of the selected S-N curve for the welded joint unique for all detail categories, Fig. 4.

$k = 1.1 - 0.35\frac{L-100}{300} = 1.015$ is the Weibull distribution shape parameter for rule length of ship L=173.15 m.

Service loading proportions of the ship's life are α_{full} = 0.5 for full load condition, α_{bal} = 0.5 for ballast condition.

μ_{Full}=0.85 and μ_{Ball}=.95 are coefficient taking into account the change in slope of the S-N curve and Γ is Gamma function.

The fatigue strength procedures [9, 10] undertake assumed operational profile, Table 2. The results provide fatigue damage assessment of lifetime service and linearly for each voyage in full and ballast conditions, respectively, Table 3.

Table 2. Load cycles and design life

25 year design lifetime		1voyage
$n_{s\ cycles}$	7.50E+7	1.0E+5
n_{sFull}	3.75E+7	5.0E+4
n_{sBall}	3.75E+7	5.0E+4
n_v voyage	750	30/year
Td years	25years	12+12 days

Table 3. Damage progression in lifetime

34 year service lifetime		1voyage
D_{Full}	0.706	4.71E-4
D_{Ball}	0.026	0.18E-4
$D=D_{Full}+D_{Ball}$	0.732	4.89E-4
n_v voyages	1021	
T=Td/D years	34years	

To achieve an acceptably high fatigue life the linear cumulative damage ratio normally should not exceed D=1. However, the rules require that the cumulative damage due to all loading conditions participating with p_j in the lifetime should be $\sum(p_j \cdot D_j) \le 0.7D$ [9]. Here, a reduced limit value of the damage ratio is required by the rules [9] because the possible additional fatigue damages due to changes between the individual load conditions are not considered. The next example investigates how the fatigue yield approach can rationally explain the discrepancy between the linear damage progression approach and practical observations on fatigue life shortening under sequences of intermittent block loadings.

FATIGUE YIELD ASSESSMENT

The merchant ship's lifetime operation is a long sequence of damage accumulations under a great number of alternating block loadings due to interchanges of full loaded and ballast seagoing conditions among a number of repairs and changes in still water, harbor and docking conditions. The operational profile, Table 2, simplifies the true complex and uncertain ship service. For a large number of block loadings the relation (15) assesses the non linear fatigue yield as an aging process superimposed to the linear damage progression over years. The additional damages are the consequence of fatigue yield due to worsening of former fatigue properties caused by interchanging of intermittent service load conditions, Fig. 11.

The effect of fatigue yield on a stiffener end welded to the side longitudinal under alternating load sequences shortens the lifetime at 80.75% of the lifetime calculated under LDR. The LDR forecast of 34 shortens at 28 years due to FYR, Fig. 11.

However, if average load variability factors as in (11) are applied, as for example v=1.1 for full load and 1.3 for ballast condition, the lifetime reduces for another 10%, that is 24 year or 0.7 of the forecasted lifetime, Fig. 11. Note how the fatigue yield correction depends only on damage progression upon appropriate IIW S-N data and doesn't depend on ship's operational profile. The corrected result closes to the rule based value for fatigue life shortening of 0.7 for uncertain intermittent block loadings [9].

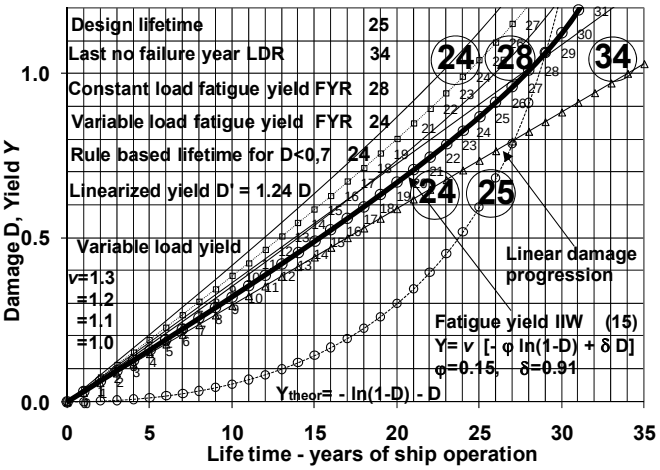

Figure 11. Fatigue yield by years of operation

The fatigue failure due to yielding of detail 2 could occur in the 24th year at the beginning of the 737th fully loaded seagoing voyage instead of the 1021st voyage in the 34th year as forecasted by LDR, Fig. 12. This fatigue life is even shorter of the anticipated rule based design lifetime of 25 years.

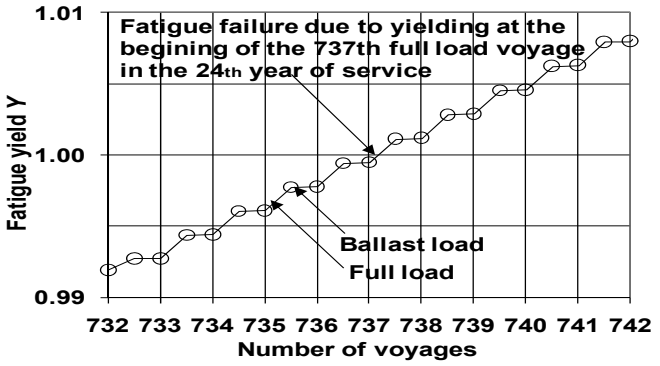

Figure 12. Fatigue yield by voyages

CONCLUSION

The study investigated the fatigue yield model on a critical intersection of a side transverse web frame stiffener end to the outer side shell longitudinal in the double hull of a tanker.

The fatigue yield traces how the fatigue damage escalates slower at the beginning and then yields more rapidly towards the fatigue failure [5]. Therefore it could be useful to start with inspections of critical structural details amidst of the expected lifetime when the fatigue yield begins to accelerate notably faster of the anticipated linear damage progression.

The deficiency of the investigation is the lack of data about load amplitude variability factors for shipbuilding steels. Therefore the factors applied in example were borrowed from earlier tests on other types of steels. However, the variable load amplitude fatigue testing methods are available and could be applied on shipbuilding steels.

The general fatigue yield approach provides parameters for adjustment of starting inclination to yielding and of yielding intensity during the lifetime. Both the parameters could be set to values appropriate to additional constant and variable amplitude block loading fatigue experimental information, environment, corrosion and inspection as well as maintenance procedures. The example employed IIW S-N data and classification rules to assess the fatigue yield parameters.

The fatigue yield approach provides distinction between numbers of variable length damaging blocks to failure [5]. High to low damaging sequences provide a fewer number of blocks to failure than the uniform and low to high sequences.

The fatigue yield model accounts for the accelerated fatigue strength deterioration and for the endurance reduction under block loadings. The non-linear fatigue yield is an accumulating aging process under a number of different loading blocks that cumulatively changes the primarily assumed fatigue properties with respect to the loading history. Thus, the non-linear fatigue yield additionally increases the fatigue damage accumulation under linear damage progression assumption and shortens the lifetime anticipated by LDR.

The fatigue yield approach undertakes the basic linear fatigue damage analysis LDR and modifies the results for the fatigue yielding and fatigue strength worsening as well as for the load variability effects by employing FYR.

The results in the paper indicate that the fatigue life of the considered critical detail of the ship hull could become shorter for about 20% due to fatigue yielding with respect to the linear damage progression model. The yielding impairs the current fatigue strength properties for formerly accumulated damages. The lifetime could shorten even more, for about 30% overall, due to load amplitude variability effects in addition to the damage progression and fatigue yielding. The calculated fatigue life shortening due to yielding and load variability effects in the paper closes to the practical observation of 30% fatigue life reduction for a number of uncertain load cases.

REFERENCES

1. Fatemi A, Yang, L. Cumulative Fatigue Damage and Life Prediction Theories: A Survey Of the State of the Art for Homogeneous Material, Int J of Fatigue 20, 1 (1998), Elsevier Science: 9-34.
2. Palmgren A. Die Lebensdauer von Kugellagern (The Life Span of Ball Bearings), Z Ver Deutsch Ing 68 (1924): 339–341.
3. Miner M.A. Cumulative Damage in Fatigue, J Appl Mech 12 (1945): 159–164.
4. Marco, S. M, Starkey, W. L. A Concept of Fatigue Damage, Trm.wc/ion,s of the ASME 76 (1954): 627-632.
5. Ziha, K. Fatigue Yield, *Int. J. of Fatigue,* Elsevier Science, 31, 7 (2009): 1211-1214 or http://dx.doi.org/10.1016/j.ijfatigue.2008.11.014 .
6. IIW, International Institute of Welding, Recommendations for Fatigue Design of Welded Joints and Components (March 2002): XIII-1539-96/XV-845-96 and (July 2004): XIII-1965-03/XV-1127-03.
7. European Convention for Constructional Steelwork: Recommendations for the Fatigue Design of Steel Structures. ECCS Publication 43, 1985.
8. Eurocode 3: "Design of Steel Structures": ENV1993-1-1: Part 1.1, General rules and rules for buildings, CEN, 1993.
9. Germanischer Lloyd, Rules & Guidance, Rules for Classification and Construction, Ship Technology. Part 1. Seagoing Ships, Chapter 1 – Hull Structures, Section 20 - Fatigue Strength, 2008, www.gl-group.com .
10. IACS International Association of Classification Societies: Common Structural Rules for Double-Hull Oil Tankers, Fatigue Strength Assessment, 2007, www.iacs.org .
11. Blagojević, B, Domazet, Ž, Žiha, K: Productional, operational and theoretical sensitivities of fatigue damage in shipbuilding, Journal of Ship Production, SNAME, Vol. 18., No. 4., 2002., pp.185-194.
12. Socha, G. Prediction of the Fatigue Life on the Basis of Damage Progress Rate Curves, Int J of Fatigue 26 (2004): 339–347.
13. Johannesson, P, Svensson, T, de Mare, J. Fatigue Life Prediction Based on Variable Amplitude Tests—Methodology, Int J of Fatigue 27 (2005): 954–965.
14. Hansen, P.F. and S.R. Winterstein. *Fatigue damage in the side shells of ships.* Marine Structures 8, Elsevier Science 1995., 631-655.
15. Committee III.2. *Fatigue and Fracture.* 13th International Ship and Offshore Structures Congress. Trondheim, Norway, 1997. 287-337.